

IMPACT PERFORMANCE AND AN
EVALUATION CRITERION FOR
MEDIAN BARRIERS

by

Hayes E. Ross, Jr.
Associate Research Engineer
Texas Transportation Institute

and

John F. Nixon
Engineer of Research
Texas Highway Department

For Presentation at the
Fifty-Fourth Annual Meeting
Transportation Research Board
Washington, D.C.
January, 1975

Texas Transportation Institute
Texas A&M University
College Station, Texas

DISCLAIMER

The contents of this paper reflect the views of the authors who are responsible for the facts and the accuracy of the data presented herein. The contents do not necessarily reflect the official views or policies of the Federal Highway Administration. This report does not constitute a standard, specification, or regulation.

KEY WORDS

Median Barriers, Crash Tests, Math Simulations, Warrants, Impact Angles, Impact Severity.

ABSTRACT

This study involved the determination of the impact performance of the Texas Metal Beam Guard Fence median barrier (MBGF) and a comparison of its performance with that of the Texas Concrete Median Barrier (CMB). The MBGF consists of two standard W-shaped guardrails mounted back-to-back on a 6 WF 8.5 support post whereas the CMB is a solid concrete barrier.

The impact performance of the MBGF was determined from a combination of crash tests and from crash simulations by the Highway-Vehicle-Object-Simulation-Model (HVOSM). Standard size automobiles were used in both the crash tests and the crash simulations. A close comparison of test and simulated results verified the accuracy of the HVOSM in simulating impacts with the MBGF. The impact performance of the CMB was obtained from another study.

Inspection of 135 median barrier impacts on various urban freeways in Texas were made to determine the distribution of impact angles. These field measurements, supplemented by data from the HVOSM, provided impact angle probabilities as a function of median widths.

The final product of this study was an evaluation criterion which provides an objective means of comparing the impact severity of the MBGF and the CMB as a function of the median's dimensions. The criterion is based on a design speed of 60 mph, and impacts with a full-size automobile.

INTRODUCTION

To prevent median crossover accidents, the Texas Highway Department (THD) uses, in most cases, one of two basic median barriers. These are the concrete median barrier (CMB) and the metal beam guardfence (MBGF). The CMB is for all practical purposes a "rigid" unyielding barrier, while the MBGF is considered to be a "flexible" barrier, one that deforms upon impact.

Several studies have been conducted to determine the impact performance of the CMB (1, 2, 3, 4, 5). It has been shown that for small impact angles the CMB can safely redirect an encroaching vehicle. However, these studies also showed that as the impact angle increases the impact severity increases considerably.

With regard to the MBGF, only a very limited amount of impact performance data existed prior to this study. One of the objectives of this study was therefore to determine its impact performance so that objective comparisons could be made between the CMB and the MBGF. Crash tests and the Texas Transportation Institute's version of the HVOSM (Highway-Vehicle-Object-Simulation-Model) computer program were used to accomplish this objective. The HVOSM was developed at CALSPAN Corporation, Buffalo, New York, for the FHWA (11). Before applying the HVOSM, however, an extensive validation study was performed. Crash test data were compared with the HVOSM predictions. Some modifications were made to the HVOSM in order to achieve an acceptable comparison.

Another task this study addressed concerned the relationship between median width and the probable angle of impact into a median barrier for

errant vehicles. This relationship was needed to develop an evaluation criterion for the two barrier systems. It has been postulated that the CMB is best for "narrow" medians where high impact angles are improbable and that the MBGF should be used for "wide" medians. However, objective criteria to quantify what "narrow" and "wide" means had to be developed. To accomplish this task, a combination of field measurements and HVOSM computer simulations was used. THD personnel conducted the field measurements. Median barriers on selected urban freeways were inspected for impact damage. Where impacts had occurred, measurements of the angle of impact, median width, etc., were made. These data were then statistically analyzed to determine impact angle probabilities. The HVOSM was used to supplement the field data by defining "upper limits" on impact angles as a function of median widths.

The end result of this study was an objective criterion which can be used in the median barrier selection process. The criterion, which is in the form of a graph, shows the relationship between impact severity and median width, on a probability basis, for the CMB and the MBGF barriers. Other factors, such as installation and maintenance costs, must of course be considered in the selection process. However, an evaluation of these factors was not within the scope of this study.

This paper summarizes the study. Full details of the study are given in a Texas Transportation Institute research report (12).

CRASH TESTS OF MBGF

Prior to the tests conducted in this study, only one full-scale crash test had been conducted on the MBGF (3, 4). In that test, an automobile impacted the barrier at 57.3 mph (92.2 km/h) at an impact angle of 25 degrees. That test was denoted "T4-1" in References 3 and 4 and is denoted the same herein.

The impact conditions of two tests conducted in this study were 60 mph (96.5 km/h) at 8 degrees, and 63.4 mph (101.4 km/h) at 14.7 degrees. These two tests and the one mentioned above provided considerable insight concerning the impact performance of the MBGF for 60 mph (96.5 km/h) impacts. The tests also provided a data base from which the HVOSM could be validated. After validation, the HVOSM was used to determine the impact performance of the MBGF at speeds below and in excess of 60 mph (96.5 km/h).

MBGF Details

The as-tested MBGF barrier is shown in Figure 1. The THD designation of the barrier is MBGF (B)-74. In some installations a 3/8 inch (9.5 mm) steel wire pedestrian control cable is placed below the guardrail. Also a headlite-barrier fence is sometimes placed on top of the barrier. However, it is assumed that neither of these features will significantly affect the impact performance of the barrier.

Upon impact the MBGF support posts break away from their base, allowing the back-to-back guardrail to deform. The 3/8 inch (9.5 mm) fillet welds connecting the outer faces of the two post flanges to the

5/8 inch (15.9 mm) base plate are designed to fracture at relatively low impact forces. Since the posts shear off at the base at a relatively low impact force, the rail does not rotate significantly, minimizing the possibility of vehicle ramping.

Crash Tests

The two crash tests conducted in the study are referred to herein as MB-1 and MB-2. The MB-1 test refers to the 60 mph (96.5 km/h) 8 degree impact and the MB-2 test refers to the 63.4 mph (101.4 km/h) 14.7 degree impact.

Test vehicles and test dummy. A 1965 Plymouth, weighing approximately 4200 pounds (18690 N), was used in Test MB-1. Figure 2 shows the vehicle prior to and after the test. A 1964 Plymouth, weighing approximately 4200 pounds (18690 N), was used in Test MB-2. Figure 3 shows the vehicle prior to and after the test. In each of the two tests a 50th percentile male dummy was placed in the driver's seat and lap belted.

Data acquisition. Crash test data were recorded by electronic instrumentation placed in the vehicle and by high speed cameras which photographed the impacts.

Three accelerometers were positioned near the center of gravity of the automobile. These accelerometers measured the longitudinal, lateral, and vertical accelerations, all with respect to a vehicle-fixed axis. The force in the dummy's lap belt during impact was measured. Also, accelerometers were placed in the dummy's chest to measure accelerations in the fore and aft direction (eyeballs in or out) as well as in the left and right (lateral) direction.

One high speed camera was positioned with a field of view parallel to the longitudinal axis of the barrier and the other camera's field of view was perpendicular to the barrier's longitudinal axis. Film speed was approximately 500 frames per second. The film provided a time history of the vehicle's motion.

Test Results

The results of Tests MB-1 and MB-2 are summarized in Table 1. Vertical accelerations were found to be small in comparison to the longitudinal and lateral accelerations and are therefore not shown herein.

Damage to the MBGF after each test is shown in Figure 4. As can be seen, damage to barrier after Test MB-1 was negligible and no repairs are necessary. Repairs to the barrier after Test MB-2 would consist of replacing two 25-foot (7.5 m) W-beam guardrails, three support posts, and the necessary bolts, nuts, etc.

Damage to the automobile after each test is shown in Figures 2 and 3. The test car in MB-1 was still operable after the test. However, damage to the left front wheel assembly of the vehicle in Text MB-2 prevented its operation after the impact.

VALIDATION OF HVOSM FOR MBGF IMPACT SIMULATIONS

The three full-scale crash tests described in the previous section provided impact performance data for the MBGF when impacted by a standard

size automobile at approximately 60 mph (96.5 km/h). It was desirable however, to obtain more data on its performance since impacts in the field could be expected to occur at speeds both below and above 60 mph (96.5 km/h).

In lieu of additional crash tests (which were not within the budget), it was decided to determine if HVOSM could simulate an automobile impacting the MBGF. To make this determination, the three MBGF crash tests (MB-1, MB-2, and T4-1) were simulated by HVOSM and the results were compared with the test results.

Validation Process

The validation process actually involved a trial and error procedure. Errors were also uncovered in an impact subroutine of HVOSM and these were corrected. Adjustments were made in the vehicle and barrier stiffness parameters until the HVOSM simulation converged on the results of the MB-2 test. However, these same stiffness parameters were used in the simulation of the other two tests (MB-1 and T4-1) and the resulting comparisons were very good. With the exception of the coefficient of friction between the vehicle and the barrier, it was not necessary to adjust parameters in each test simulation. As a consequence, it was felt that these parameters could be used in HVOSM to simulate impacts with the MBGF at speeds above and below 60 mph (96.5 km/h).

With regard to the vehicle-barrier friction coefficient, it was found that its value had to be adjusted upward as the angle of impact increased. This increase was necessary to simulate the effects of the slight "pocketing" which occurred, i.e., pocketing of the vehicle by

the barrier.

Comparisons Between HVOSM and Tests

Comparisons between HVOSM and the test results were made on two basic types of data. These were accelerations at the vehicle's center of gravity (C.G.) and vehicle motion.

Vehicle motion comparisons. Figure 5 shows a comparison of test and simulation of vehicle motion for the MB-1 test. Similar plots were made for the other two tests. The HVOSM perspective drawings were generated by a computer program (6) whose input is the HVOSM output. Hidden lines were removed from the perspective drawings by hand for clarity. The test photos are prints made from selected high speed film frames. It can be seen that the general motion of the HVOSM compares well with the test results. Note that the automobile does not roll appreciably after impact with the MBGF, as was the case in all three tests.

Acceleration comparisons. Figure 6 shows a comparison of test and simulation lateral acceleration for Test MB-1. Similar comparisons were made for the other two tests. Comparisons were also made between test and simulation longitudinal accelerations.

The HVOSM accelerations generally followed the trend of the test accelerations. In some instances the test data were characterized by rapid changes while the HVOSM values were somewhat smoother. This high-frequency vibratory nature of the test data is attributed in part to "ringing" or high-frequency response of the sprung mass of the

vehicle. HVOSM does not have the capability to simulate this type of response. However, the contribution of such accelerations to overall impact severity is not considered significant. Another reason for sudden and large changes in the test values is that as the vehicle crushes, various members of various stiffnesses are encountered. HVOSM can simulate this effect to a small degree by "hard points".

A summary of the acceleration data is given in Table 2. Shown in the table are peak accelerations and the highest average accelerations occurring over any 50 millisecond period. The times at which the peak accelerations occur and the periods over which the highest average accelerations occur are also given in the table.

Although some disparity occurs between test values and the HVOSM values for peak accelerations and the times at which these occur, the average accelerations are in reasonably close agreement. In most cases, more significance is placed on the highest average accelerations rather than the highest peak accelerations. This is especially true when vehicle accelerations are used as a measure of severity (to the occupant/occupants of the vehicle).

After evaluating the validation efforts, it was concluded that HVOSM (as modified) could be used to supplement crash test data for the MBGF. When considering the very complex nature of the MBGF impacts, HVOSM predicted the gross motion of the vehicle and vehicle accelerations quite accurately.

PARAMETRIC STUDIES

Metal Beam Guard Fence

To supplement the MBGF crash test data, nine HVOSM simulations were made. Impacts at speeds of 50 mph (80.5 km/h), 70 mph (112 km/h), and 80 mph (128 km/h), in combination with impact angles of 5 degrees, 15 degrees, and 25 degrees, were simulated.

Table 3 summarizes the results of these nine simulations (runs 1 through 9). Also shown in Table 3 are the results of the simulations of the three crash tests (runs 10, 11, and 12). The accelerations given in Table 3 are the highest average accelerations occurring over any 50 millisecond period. A small utility computer program was written to compute these maximum averages as well as the maximum severity index (discussed in a following paragraph). The program scanned the data, computed the average accelerations and the severity index for all 50 millisecond periods, and selected and printed the maximums. It is noted that the time period over which the maximum average longitudinal acceleration occurred did not necessarily correspond to that for the average lateral acceleration. Also, the time period over which the maximum severity index occurred did not necessarily correspond to that for the maximum average longitudinal acceleration or to that of the maximum average lateral acceleration.

A severity index (S.I.) was used to quantify the severity (to an occupant) of the vehicle impacts with the MBGF. It is defined as follows (7):

$$S.I. = \sqrt{\left(\frac{G_{Long}}{G'_{Long}}\right)^2 + \left(\frac{G_{Lat}}{G'_{Lat}}\right)^2 + \left(\frac{G_{Vert}}{G'_{Vert}}\right)^2} \quad (1)$$

Where

- G_{Long} = average longitudinal acceleration;
- G_{Lat} = average lateral acceleration;
- G_{Vert} = average vertical acceleration;
- G'_{Long} = tolerable average longitudinal acceleration;
- G'_{Lat} = tolerable average lateral acceleration; and
- G'_{Vert} = tolerable average vertical acceleration.

The terms in the numerator of Equation 1 are the average accelerations of the vehicle, and the terms in the denominator are the limiting vehicle accelerations an occupant can withstand without serious or fatal injuries. It is assumed that an S.I. greater than one indicates that an occupant would sustain serious or fatal injuries. A detailed description of the index is given in the literature (7, 8).

Limiting accelerations used in this study were as follows (7):

- $G'_{\text{Long}} = 7$
- $G'_{\text{Lat}} = 5$
- $G'_{\text{Vert}} = 6$

For the MBGF, the vertical accelerations were negligible and therefore only the first two terms of the S.I. were included. However, the severity indices on the CMB (provided in subsequent parts of this report) involved all three terms since all three acceleration components were significant.

Concrete Median Barrier

In the following section, the S.I. for the MBGF is compared with

that of the CMB. Values of the S.I. for the CMB were obtained from a previous study (1, 2), with two exceptions. To adequately compare the two barriers, it was necessary to simulate two impacts with the CMB which were not in the previous study. Impacts at 50 mph (80.5 km/h) and 25 degrees and at 70 mph (112 km/h) and 25 degrees were simulated. The results of these two runs, together with all other CMB data, are given in Table 4.

COMPARISON OF CMB AND MBGF IMPACT PERFORMANCE

Impact Severity

Shown in Figure 7 are plots of the S.I. versus impact speed for the CMB and the MBGF for three different impact angles. Data in Figure 7 were taken from Tables 3 and 4.

It can be seen that for small impact angles, the two barriers are approximately equal in impact severity. However, as the impact angle increases, the difference in impact severity of the two barriers is more pronounced, with the MBGF providing the less severe impact. This result was expected since the MBGF does have flexibility and can dissipate a considerable amount of the energy of the impacting vehicle. The CMB is for all practical purposes a rigid barrier.

It can be seen from Table 3 that the MBGF can redirect a vehicle without introducing large roll angles, i.e., the potential for roll over appears to be minimal. This could be a significant factor when comparing the MBGF with the CMB since at high speeds and large impact angles the

latter has shown a tendency to cause the impacting vehicle to roll over (2).

Damage Costs

Evaluation of the impact performance of a barrier should include a consideration of repair costs to both the barrier and the vehicle. The following cost figures, which admittedly are based on very limited data, give a quantitative measure of the damage costs incurred after impact with the MBGF and the CMB.

With regard to barrier damage, the CMB requires no repair for all practical purposes, at least for the impact conditions investigated. Damage to the MBGF for an impact at 60 mph (96.5 km/h) and an impact angle of 7 degrees was negligible. Damage to the MBGF for 60 mph (96.5 km/h) impacts at impact angles of 15 degrees and 25 degrees is approximately the same. Repair cost in these cases is based on previous estimates (3) with a factor of 1.2 being applied to estimate cost increases since the referenced data were published. The barrier repair costs are shown in Table 5.

Also shown in Table 5 are the estimated costs to repair the automobiles after impact with the respective barriers. Automobile repair costs were obtained in each case from a local auto appraiser.

Based on the estimates and the corresponding impact conditions, impact with the CMB will cause more damage to the automobile than the MBGF. However, it is pointed out that at impact angles less than 7 degrees, the CMB will redirect an automobile with little or no sheet

metal damage, which reduces or eliminates damages. The MBGF does not have this capability and some automobile damage can be expected for any impact.

IMPACT ANGLE PROBABILITIES

The study up to this point provided objective criteria for comparing the impact performance of the CMB and the MBGF for a given set of impact conditions, i.e., impact speed and angle. However, data in this form are of limited value if one cannot relate impact conditions (or probability thereof) to the particular median geometry in question. The objective of this phase of the study was therefore to determine the impact angle probability as a function of median width or the distance from the roadway to barrier's face.

To accomplish this objective, the researchers relied on both field data and on data as determined by use of the HVOSM model. A description of each of these two approaches follows.

Field Data on Barrier Impacts

Very valuable work on the nature of vehicle encroachments has been done by Hutchinson and Kennedy (9). However, the referenced work involved all encroachments and there was no apparent way to predict what number of these encroachments would have impacted a barrier, had there been one in the median, and at what impact angle. It was decided that a number of field evaluations would be made to determine actual impact angles.

The field data were gathered by members of the THD Research Division. The field sites were urban freeways of several large cities in Texas. The collection procedure involved the location of sites where median barrier accidents had occurred (as judged by barrier damage) in which impact angles could be measured, either through skid marks or tire tracks. In some cases, the barrier deflection (permanent set) was measured. However, there was no attempt to relate barrier damage to any other parameters, such as vehicle speed.

Median widths investigated ranged from 13 feet (3.9 m) to 56 feet (16.8 m). A total of 135 cases were recorded. However, a large portion of these (111) were in the 22-foot (6.6 m) to 26-foot (7.8 m) median width range. In a few instances, the barrier was located on a raised median. However, in such cases a roll curb was used and as a consequence it is doubtful that, as such, it would have a significant effect on the vehicle's path, at least for the short distances between the curb and the barrier.

Inspections of impacts with barriers on narrow raised medians were also made by the THD investigation team. The following statement by Hustace of the THD concerns this phase of the inspection.

"The narrow median, although sustaining numerous impacts, had frequently not provided tire tracks due to the airborne tire after having struck the curb face. Although curb scuff marks and barrier damage is usually readily apparent, the nearness of the barrier face and overhang of the vehicle would normally result in an over conservative angle from a calculated value. This factor, combined with the extreme hazard of angle measurements on narrow medians, leads me to feel that the data generated by Hutchinson and Kennedy for vehicle departure angles should be adequate to represent the narrow median situations since vehicle-driver recovery-response would be minimum due to the close proximity of the barrier. Also, in turn, the absence of wide median

barrier sites and the lack of serious consideration for median barrier installations in the wide median does not demand the same urgent attention as does the barrier installation for the medium and narrow width medians."

A statistical analysis of the 135 cases led to the following conclusions:

- (a) There was enough data to determine a relation between impact angle and probability of occurrence for median widths between 22 feet (6.6 m) and 26 feet (7.8 m). The relation is shown in Figure 8. Note that the data from the 22-foot (6.6 m), 24-foot (7.2 m), and 26-foot (7.8 m) medians were combined to develop this curve. There was not a significant variation in the distribution to warrant a curve for each of these four widths.
- (b) There was not enough data to develop distributions of impact angles as a function of median widths. This was due to the fact that most of the data was for median widths between 22 feet (6.6 m) and 26 feet (7.8 m).
- (c) Based on the data for the 22-foot (6.6 m) to 26-foot (7.8m) medians, it appears that the distribution of impact angles for a given median width can be approximated by the "normal distribution". The mean impact angle for the data was 10.8 degrees with a standard deviation of 6.2 degrees. It can be seen in Figure 8 that a normal distribution having a mean impact angle of 10.8 degrees and a standard deviation of 6.2 degrees correlates well with the field data.

HVOSM Simulations of Encroachment Angles

A series of HVOSM runs were conducted to supplement the field data. The objective of these runs was to develop relationships between encroachment angle and median width for different probability levels.

The research approach and its rationale were as follows:

- (a) The HVOSM was used to establish extreme encroachment angles (95th percentile values) for any given median width. Further details of the procedure used to determine these angles are given in a subsequent part of this section.
- (b) Using the extreme angles from part "a" and assuming a zero impact angle at the 5th percentile, a normal distribution was constructed for various median widths (a normal distribution is uniquely defined, given any two points on the curve). Use of the normal distribution in this manner appears reasonable due to its close correlation with field data (see Figure 8).
- (c) From the data generated in part "b", curves were drawn depicting impact angle versus median width for different levels of probability.

It is important to note that the ability of the HVOSM to simulate an automobile during steering maneuvers has been demonstrated by other researchers (11).

Extreme encroachment angles. Much speculation has occurred concerning the highest angle an automobile can impact a barrier located a given distance from the roadway. This investigation did not provide data to end all speculations, nor did it purport to, but it did shed some light on the problem.

Basically, the HVOSM was used to determine the response and the encroachment angle of a standard automobile with standard tires as it was suddenly steered off the roadway while travelling at 60 mph. The automobile was assumed to be in a "coast" mode, i.e., with no traction after the steering maneuver began. The maneuver consisted of steering from a zero steer angle to a prescribed angle in a prescribed time at a uniform rate. The turning rate was determined by observing the highest rates at which drivers had performed similar maneuvers in full-scale tests at TTI.

Four steering angle limits were simulated in the HVOSM. These were 4, 8, 12, and 16 degrees. The steer angle was increased up to a selected limit at a constant rate and then held constant. It is noted that most automobiles have a steering wheel angle to steer angle ratio between 20 and 25. For example, an eight-degree steer angle would require between 160 and 200 degrees of steering wheel turn.

A total of 12 simulation runs were made. For each of the four steering conditions described above, three tire-pavement friction coefficients were simulated, namely 1.0, 0.75, and 0.5. The results were presented in two basic forms; plots of the vehicle path and plots of encroachment angle versus lateral distance.

Figure 9 shows plots of the path of the center of gravity of the vehicle for a tire-pavement friction coefficient of 1.0 for the four steering angles. The "lateral distance" is a distance from the roadway tangent on which the steering maneuver began (roadway parallel to "longitudinal distance" axis). Note that an increase in the steer angle does not result in a proportionate increase in the path curvature,

especially beyond steer angles of eight degrees. This is due primarily to the saturation of the side force capabilities of the front tires after the steer angle exceeds approximately 8 degrees. It is conjectured that the curvature approaches a limiting value for steer angles of 16 degrees. It is possible that other forms of steering input (e.g., nonlinear rates of steer application) could result in paths of larger curvature, but it is doubtful that the differences would be significant.

Also shown on Figure 9 is a path plot of the vehicle as simulated by a simple "point mass" model. It can be shown that the minimum radius, r_{min} , a point mass can follow is given by:

$$r_{min} = \frac{v^2}{g\mu}$$

where

v = velocity of point mass,

μ = friction coefficient, and

g = gravitational acceleration.

From Figure 9, it can be seen that the actual paths (as determined by HVOSM) differ considerably from that of the point mass. This is due to the inability of the point mass model to accurately represent the transient nature of vehicle handling. Whereas the point mass model assumes an instantaneous steady state turn once the turn has been initiated, the HVOSM accounts for the transient period of the vehicle's response.

Shown in Figure 10 are encroachment angles as a function of lateral distance. Coordinates of each of these curves were determined by

computing the arctangent of the slope of the appropriate curve in Figure 9 as a function of lateral distance. The encroachment angle is the angle between a tangent to the C.G.'s path and the roadway tangent.

It is interesting to note that although the point mass model does not accurately simulate the vehicle's path, it does predict the encroachment angle quite accurately, at least for the extreme steering maneuvers simulated and for lateral distances up to about 40 feet (12 m). For lower friction coefficients, the comparison was found to be even better. It is also interesting to note that many people felt that the point mass representation gave very excessive encroachment angles, i.e., the vehicle could not attain the angles predicted by the point mass model. Such is not the case. In fact, for high skid-resistant pavements where large lateral distances are accessible, e.g., a wide median, the results indicate that the point mass predictions are too low.

To arrive at a relationship between extreme encroachment angle and median width (lateral distance), the values as determined for a steer angle of 16 degrees and a friction coefficient of 1.0 were selected. In most cases these conditions would be extreme and as such they represent what is considered to be "limiting" values.

Figure 11 shows the relationship between the extreme impact angle and the median distance, D , for two conditions; impact from lane 1 and impact from lane 2. Note the median distance, D , is not the half-median width but rather is the distance from the edge of the roadway to the barrier face. It was assumed that the vehicle was in the center of the 12-foot (3.6 m) lane when the emergency steering maneuver began. The curves of Figure 11 were determined from Figure 10, with slight adjustments being made to account for the dimensions of a typical

automobile (see page 59 of reference 12).

Note that the "impact from lane 1" curve will intersect the vertical axis above zero for a zero median distance, i.e., there can be an impact angle even though there is no median distance. This is due to the assumed three-foot gap between the vehicle and the face of the barrier for a vehicle travelling in the center of the lane.

Impact angle probabilities. The probability distribution of impact angles for a given median distance was assumed to be a normal distribution, as has been discussed earlier. To determine the distribution for a given median distance, the 95th percentile value of the impact angle was assumed to be that as determined from the "lane 1" curve of Figure 11 and the 5th percentile impact angle was assumed to be zero. These two points uniquely defined the distribution for any given median distance.

The decision to use these particular percentile values was arrived at through a trial and error procedure. Different combinations were tried and the distributions were compared with the field data. It can be seen in Figure 12 that the predicted distribution (theoretical) compares reasonably well with the actual field data, for a median distance of 12 feet (3.6 m) (median width of approximately 24 feet (7.2 m)). Although there are some differences in these two curves, the degree of correlation is considered to be good.

There are several factors which likely contributed to the differences that did occur in the curves of Figure 12. The first of these, and probably the most significant one, is the speed of the impacting vehicle. Unfortunately, there was no way to determine impact speeds

from the field measurements. It is conjectured that the low angle impacts occurred at speeds higher, on an average, than did the higher angle impacts. It is also conjectured that most of the impacts occurred at speeds less than 60 mph (96.5 km/h). The theoretical distribution is based on an initial encroachment speed of 60 mph (96.5 km/h). Some slight decrease in speed occurred in the HVOSM simulations during the encroachment, but it was not considered significant (less than 2 mph (.2 km/h)).

Another factor which could cause differences is that some of the barrier impacts likely occurred after the vehicle impacted another vehicle or object. Actions of the driver during the encroachment, such as braking, could also have a significant effect on the vehicle's path.

The number of lanes can also have an effect on the distribution of encroachment angles. The field data were taken on urban freeways having various numbers of lanes. As assumed, the theoretical distributions were based on encroachments from the inside lane.

It was concluded, however, that the effect of the combination of these factors could be represented by the as-formulated theoretical distribution.

EVALUATION CRITERION

Impact performance data and impact angle data needed to formulate an evaluation criterion were now available. The criterion is based on a

design speed of 60 mph (96.5 km/h) and relates to full-size automobiles. Shown in Table 6 are values of the severity index as related to impact angle. These values were obtained from Figure 7. The criterion is presented graphically in Figure 13. Coordinates of the S.I. versus impact angle curves were taken from Table 6 and the plots of median distance versus impact angle were determined from the assumed normal distributions.

It is pointed out that the criterion referred to is based on safety considerations only and does not include cost and maintenance factors. It is also pointed out that the criterion is dependent on the design speed. For example, if the design speed were 50 mph (80.5 km/h), the severity curves of Figure 13 for the two barriers would have been closer together. However, at lower design speeds, higher impact angles can be expected and the impact angle distribution curves would have to be determined for the lower speeds.

Figure 13 allows one to objectively compare the impact severity of the two barriers as a function of the median distance. For example, assume that one is interested in the impact severities of the two barriers when placed 12.5 feet (3.8 m) from the roadway (a median width of approximately 25 feet (7.5 m)), for the 80th percentile impact. Application of the curves is as shown on Figure 13. The results are as follows:

MBGF	$\frac{S.I.}{0.90}$
CMB	1.09

The results indicate the MBGF to be about 21 percent less severe for the given conditions.

As mentioned previously, the selection process involves the consideration of other factors, such as initial and maintenance costs of the barrier and the hazard to repair crews and motorists while the barrier is being serviced. It is the author's belief that a selection procedure based on a "cost-effective" analysis can be formulated which incorporates the effects of all these factors. Such a formulation, however, was not within the scope of this work.

The Texas Highway Department used the results of this study to establish guidelines for the selection of median barriers. These guidelines were also determined through careful consideration of other factors such as maintenance costs, safety to maintenance crews who must repair the barriers, and to the disruption of traffic during repairs. The guidelines are shown in Table 7.

CONCLUSIONS

The following conclusions were drawn as a result of this study:

1. The Texas standard metal beam guardfence will contain and redirect an automobile impacting at 60 mph (96.5 km/h) at impact angles of 7 degrees, 15 degrees, and 25 degrees. There is no tendency for the automobile to become unstable after impact with the MBGF and the exit angle of the vehicle is not large. Serious or fatal injuries are not predicted for impacts at angles less than 15 degrees and speeds less than 60 mph (96.5 km/h).
2. The as modified version of the HVOSM can be used to simulate automobile

impacts with the MBGF. Close correlations between test and simulated results forms a basis for this conclusion.

3. The severity of impact with the Texas standard concrete median barrier at 60 mph (96.5 km/h) is approximately equal to that of the MBGF for angles of impact of 7 degrees or less. However, as the angle of impact increases, impacts become progressively more severe with the CMB than with the MBGF.
4. The CMB is practically maintenance free whereas it costs approximately \$500 to repair the MBGF after a 60 mph (96.5 km/h), 15 degree, impact. Based on gross estimates, automobile repair costs resulting from an impact with the CMB are slightly higher than that for the MBGF at an impact speed of 60 mph (96.5 km/h) and an impact angle in excess of 7 degrees.
5. Sufficient field data was obtained to determine the percentile distribution of impact angles for a barrier placed in the center of a 24-foot median. A theoretically derived distribution, obtained by application of the HVOSM, compared favorably with the field data. Percentile distributions of impact angles as a function of median distance (distance from roadway edge to barrier face) were obtained by the theoretical analysis.
6. An objective barrier evaluation criterion was developed from which the impact severity of the MBGF and the CMB can be determined for any given median distance. The criterion is based on a design speed of 60 mph (96.5 km/h) and impacts with a full-size automobile. The Texas Highway Department used this criterion to develop warrants for the use of these two barriers.

ACKNOWLEDGEMENTS

This study was sponsored by the Texas Highway Department, in cooperation with the Federal Highway Administration. Several people provided valuable input to this study, for which the authors are very appreciative. The guidance and suggestions of Mr. Dave Hustace of the Texas Highway Department and Mr. Edward V. Kristaponis of the Federal Highway Administration are acknowledge. The field data on barrier impacts were collected and synthesized by Mr. Dave Hustace, Mr. Paul Tutt, and other members of Division 10 of the THD. Dr. Larry Ringer, Associate Professor of Statistics, Texas A&M University, provided guidance in the statistical analysis of the field data on barrier impacts.

REFERENCES

1. Young, R. D., Post, E. R., Ross, Jr., H. E., and Holcomb, R. M., "Simulation of Vehicle Impact with the Texas Concrete Median Barrier- Volume One, Test Comparisons and Parameter Study", TTI Research Report 140-5, Texas A&M University, College Station, Texas, June 1972.
2. Young, R. D., Post, E. R., and Ross, Jr., H. E., "Simulation of Vehicle Impact with Texas Concrete Median Barrier: Test Comparisons and Parameter Study", Highway Research Record No. 460, HRB, 1973, pp. 61-72.
3. Hirsch, T. J., Post, E. R., and Hayes, G. G., "Vehicle Crash Test and Evaluation of Median Barriers for Texas Highways", TTI Research Report 146-4, Texas A&M University, College Station, Texas, September 1972.
4. Post, E. R., Hirsch, T. J., Hayes, G. G., and Nixon, J. F., "Vehicle Crash Test and Evaluation of Median Barriers for Texas Highways", Highway Research Record No. 460, HRB, 1973, pp. 97-113.
5. Lundstrom, L. C., Skeels, P. C., Englund, B. R., and Rogers, R. A., "A Bridge Parapet Designed for Safety", Highway Research Record No. 83, HRB, 1965, pp. 169-183.
6. Theiss, C. M., "Perspective Picture Output for Automobile Dynamic Simulation", CAL Report No. VJ-2251-V-2R, Cornell Aeronautical Laboratory, December 1968.
7. Weaver, G. D., and Marquis, E. L., "The Relation of Side Slope Design to Highway Safety (Combination of Slopes)", Final Report on NCHRP Project 20-7, Task Order No. 2/2, Report RF 626B, Texas Transportation Institute, Texas A&M University, October 1973.
8. Ross, H. E., Jr., and Post, E. R., "Criteria for Guardrail Need and Location on Embankments, Volume I: Development of Criteria" Research Report 140-4, Texas Transportation Institute, Texas A&M University, April 1972.
9. Hutchinson, J. W. and Kennedy, T. W., "Medians of Divided Highways- Frequency and Nature of Vehicle Encroachments", Univ. of Ill. Engineering Experiment Station Bulletin 487, Urbana (1966).
10. Selby, S. M., "Standard Mathematical Tables" (CRC), Student Edition, 17th Edition, The Chemical Rubber Company, 1969, pages 581-588.
11. McHenry, R. R. and Deleys, N. J., "Vehicle Dynamics in Single-Vehicle Accidents-Validation and Extension of a Computer Simulation", Cornell Aeronautical Laboratory Report No. VJ-2251-V-3, December 1968.
12. Ross, H. E., Jr., "Impact Performance and a Selection Criterion for Texas Median Barriers", TTI Research Report 140-8, Texas A&M University, College Station, Texas, April 1974.

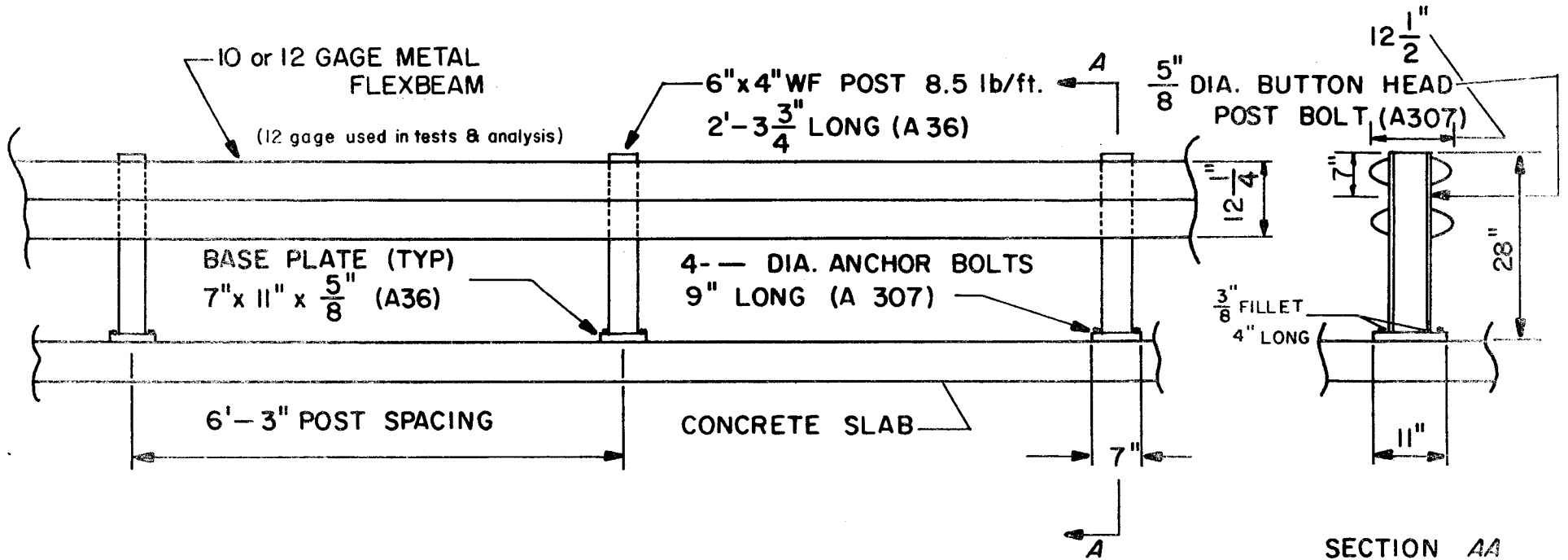


FIGURE 1. TEXAS HIGHWAY DEPT. METAL BEAM GUARD FENCE
(BARRIER) MBSF (B) - 74

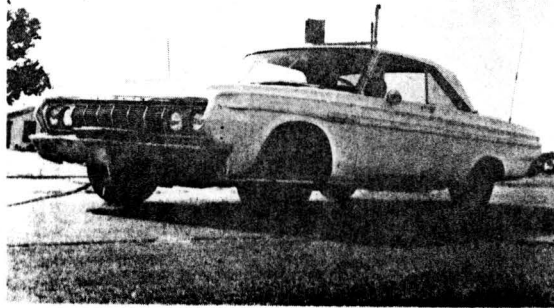


BEFORE TEST



AFTER TEST

FIGURE 2. MB-1 TEST VEHICLE

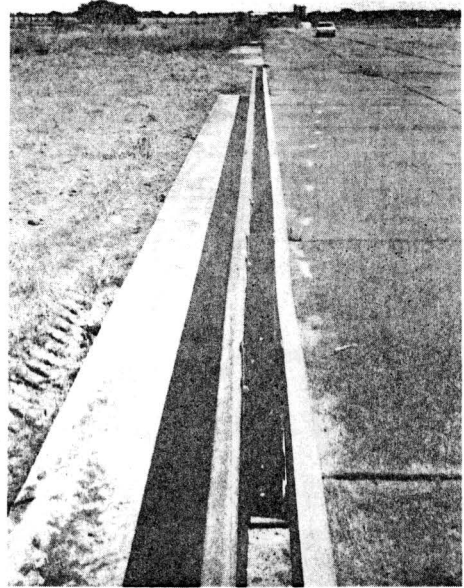
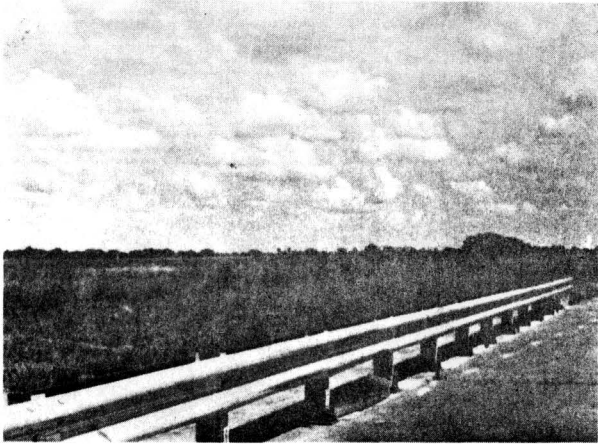


BEFORE TEST

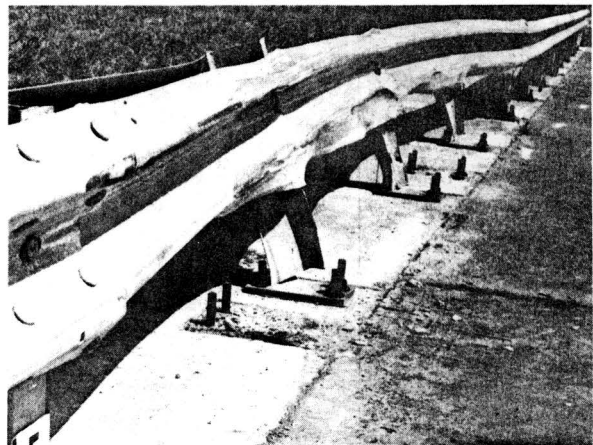
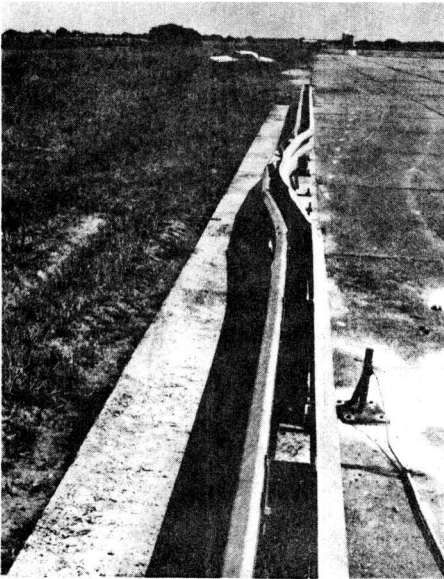


AFTER TEST

FIGURE 3. MB-2 TEST VEHICLE



AFTER MB-1 TEST

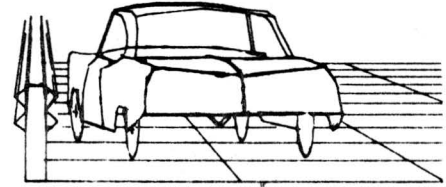


AFTER MB-2 TEST

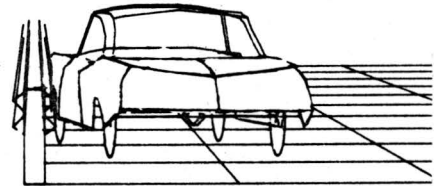
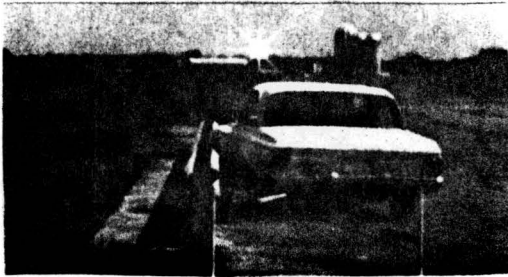
FIGURE 4. MBSF DAMAGE

TEST

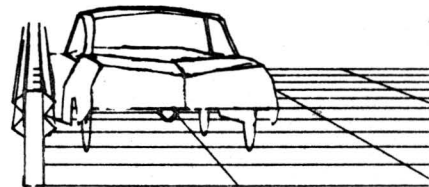
HVOSM



SEC. 0.000



SEC. .050

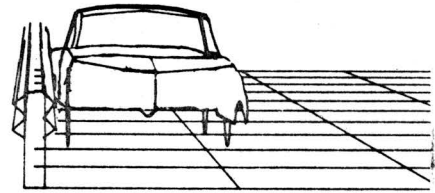


SEC. .100

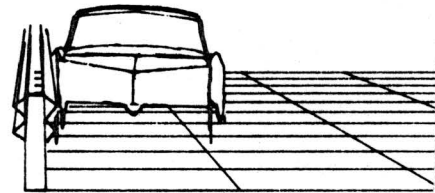
FIGURE 5. TEST VERSUS HVOSM, TEST MB-1

TEST

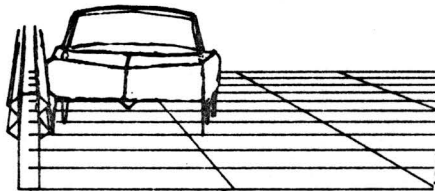
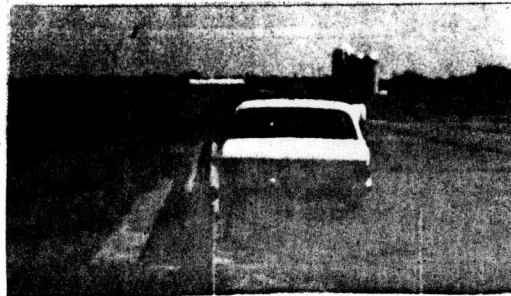
HVOSM



SEC. .150



SEC. .200



SEC. .250

FIGURE 5. CONCLUDED

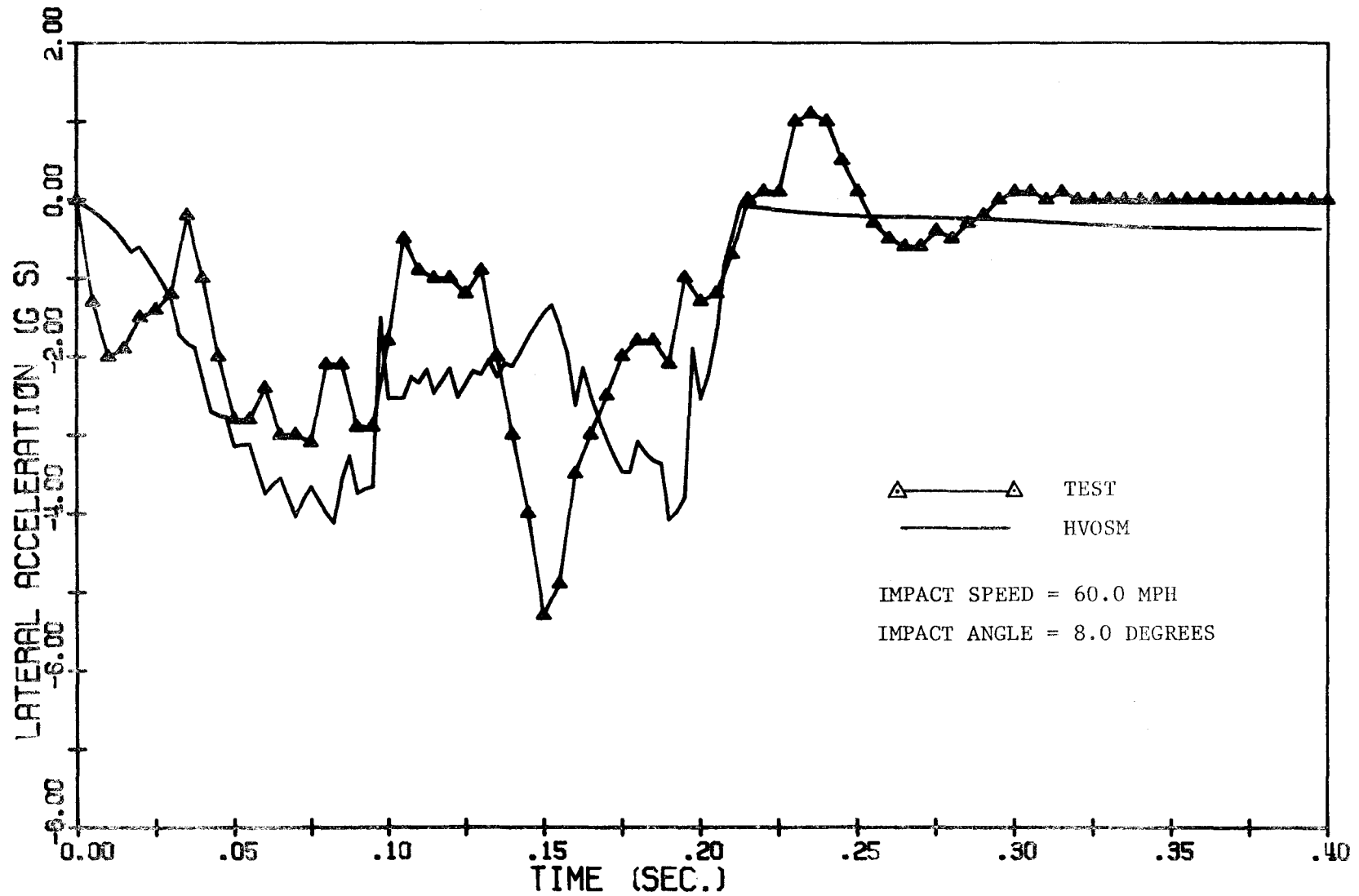


FIGURE 6. LATERAL ACCELERATION, TEST MB-1

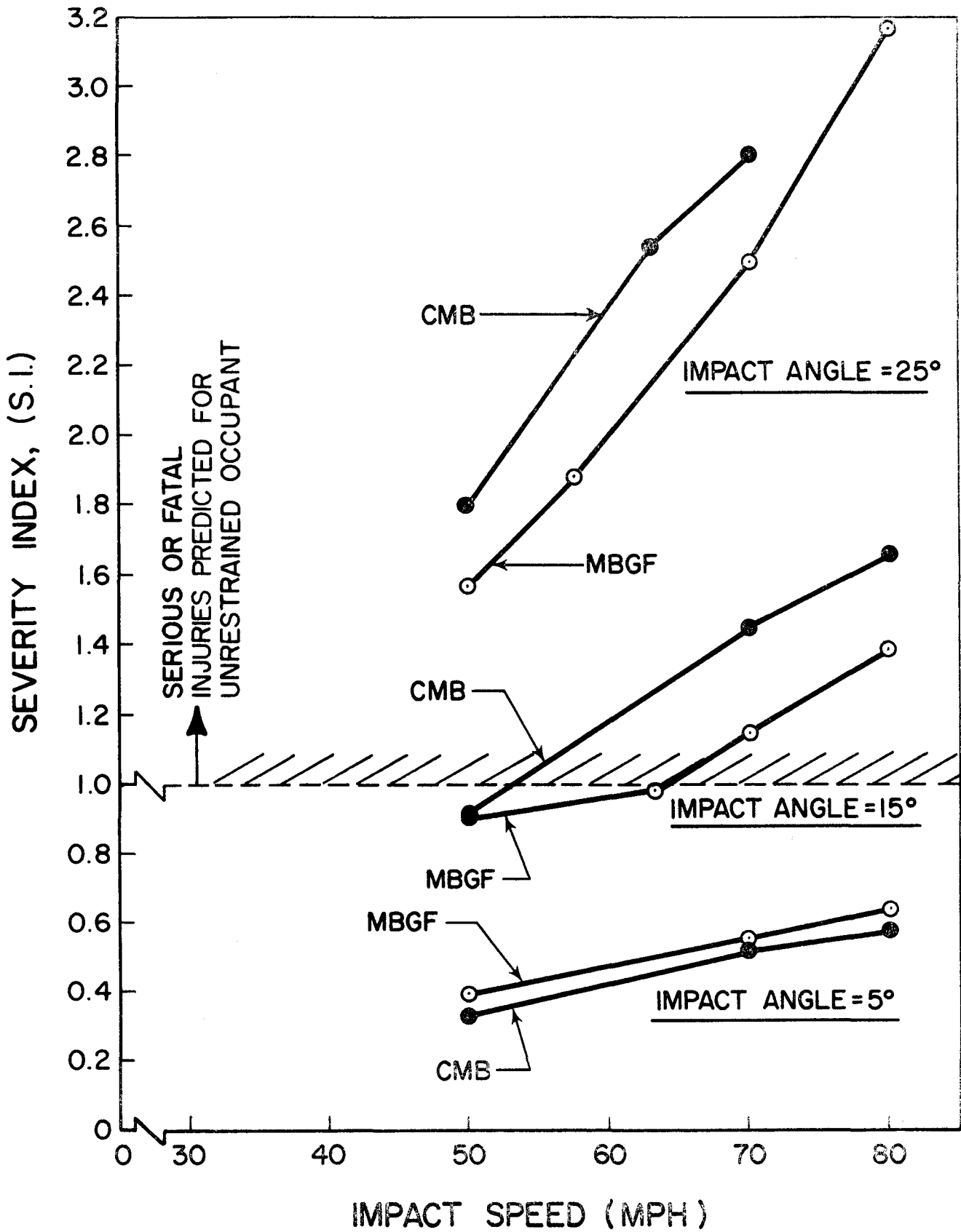


FIGURE 7. S. I. VERSUS IMPACT SPEED

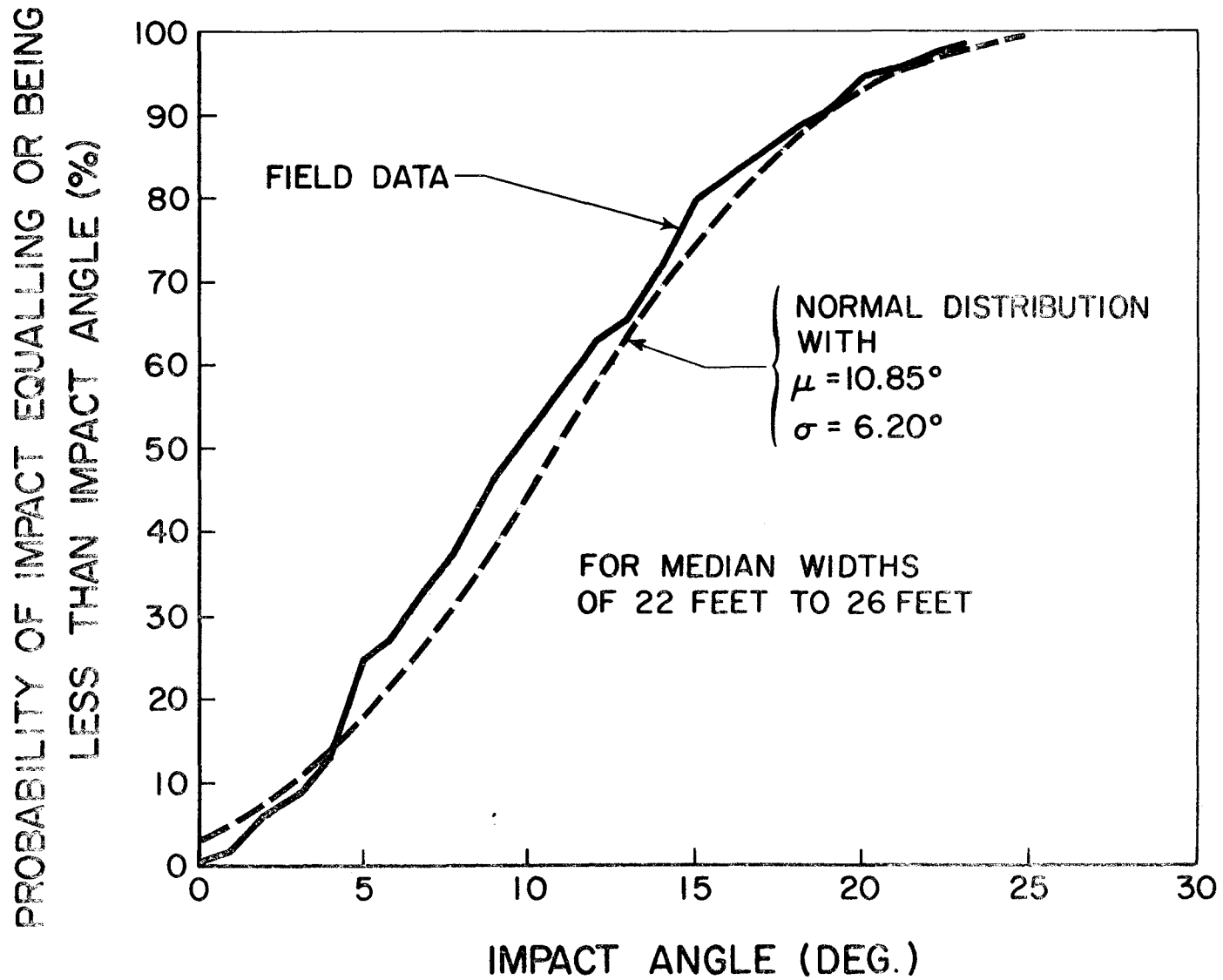
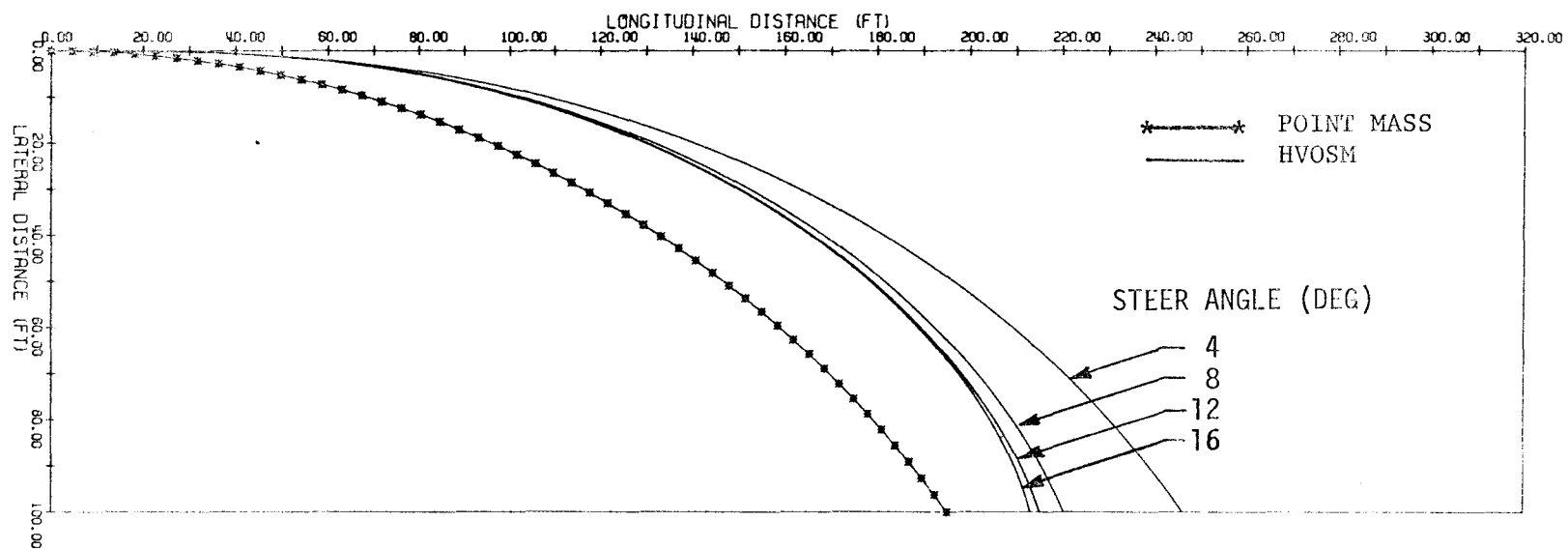


FIGURE 8. DISTRIBUTION OF IMPACT ANGLES FOR FIELD DATA

FIGURE 9. VEHICLE PATH, $\mu = 1.0$

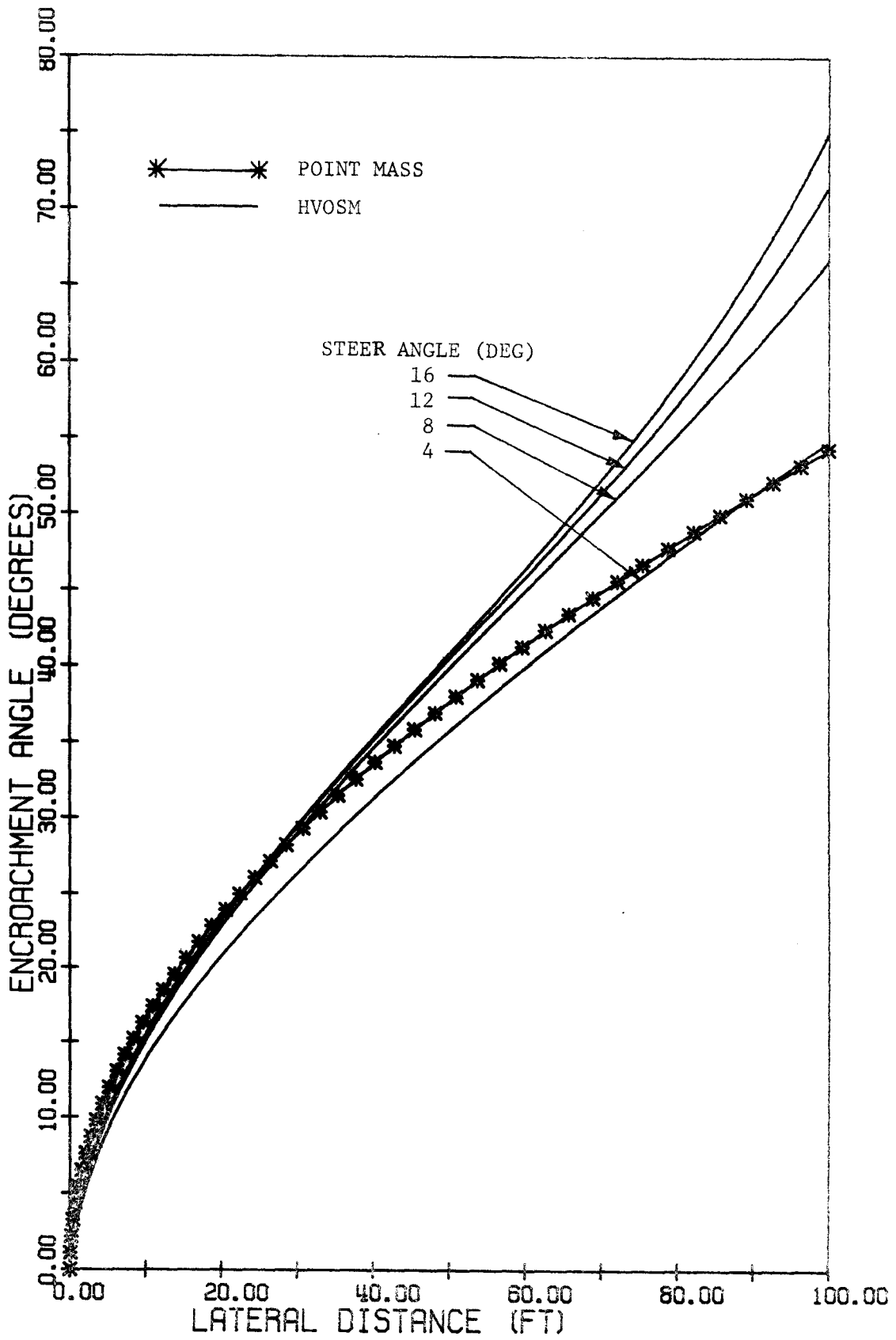


FIGURE 10. ENCROACHMENT ANGLES, $\mu = 1.0$

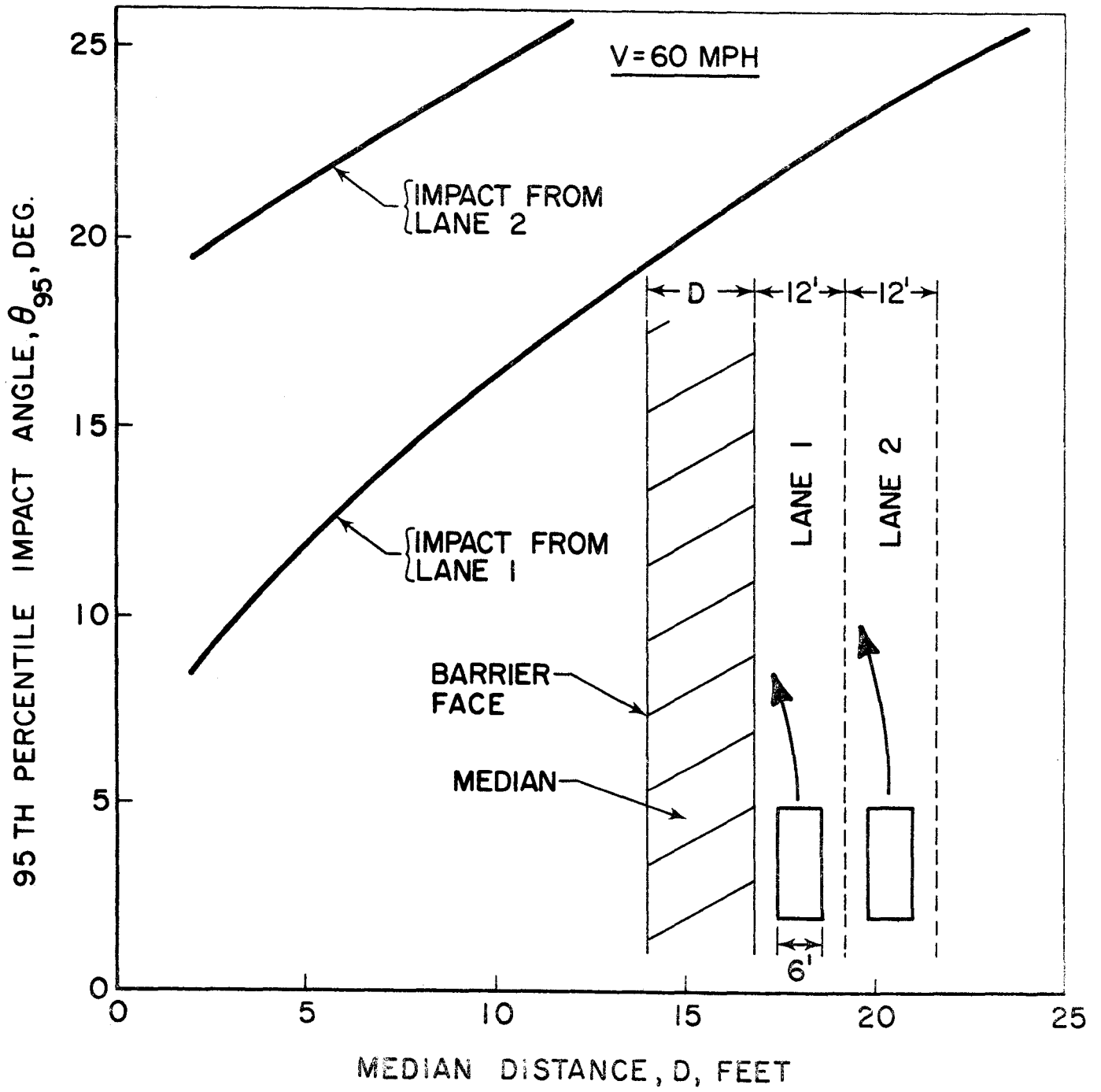


FIGURE 11. NINETY - FIFTH PERCENTILE IMPACT ANGLE
VERSUS MEDIAN DISTANCE

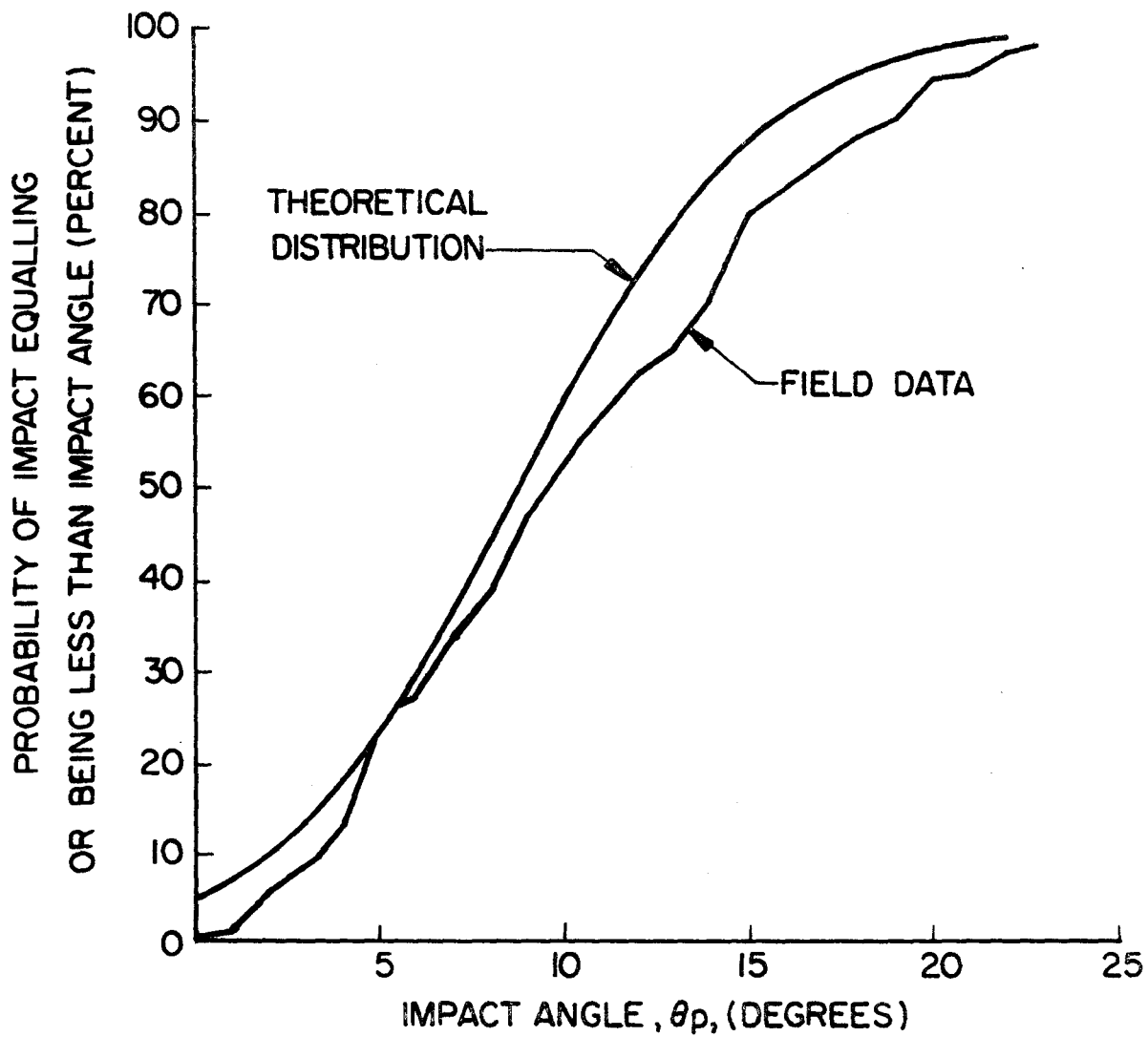


FIGURE 12. IMPACT ANGLE VERSUS PROBABILITY OF IMPACT, MEDIAN DISTANCE = 12 FEET

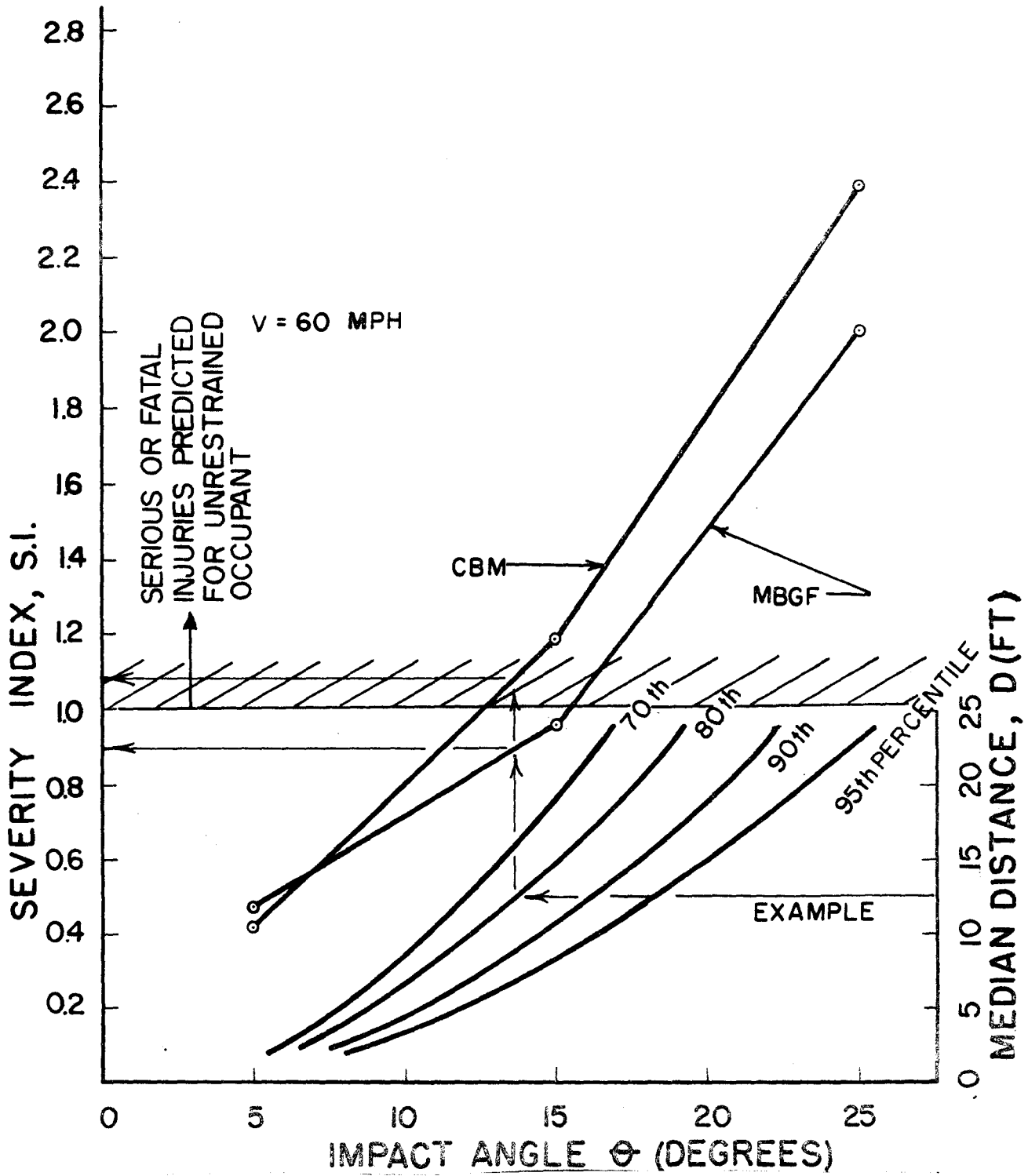


FIGURE 13. EVALUATION CRITERION

TABLE 1. SUMMARY OF MBGF TESTS

DATA	TEST NUMBER			
	MB-1		MB-2	
<i>VEHICLE</i>				
Year	1965		1964	
Make	Plymouth		Plymouth	
Weight (lb)	4200		4200	
<i>FILM DATA</i>				
Impact Speed (mph)	60.0		63.4	
Impact Angle (deg)	8.0		14.7	
Dynamic Barrier Deflection (in.)	1.0		12.0	
Departure Angle (deg)	4.0		3.8	
Departure Speed (mph)	47.0		52.0	
<i>ACCELEROMETER DATA</i>				
	VEHICLE	DUMMY	VEHICLE	DUMMY
Longitudinal				
Peak (G's)	2.0	5.3	5.5	5.4
Highest Average (G's) ¹	0.03	4.2	0.90	4.3
Lateral				
Peak (G's)	5.3	4.0	7.0	8.2
Highest Average (G's) ¹	3.2	2.9	4.7	6.3

¹ Averaged over 50 milliseconds.

TABLE 2. ACCELERATION COMPARISONS

	TEST NUMBER					
	MB-1		MB-2		T4-1*	
	<u>Test Results</u>	<u>HVOSM Results</u>	<u>Test Results</u>	<u>HVOSM Results</u>	<u>Test Results</u>	<u>HVOSM Results</u>
Peak Lateral Acceleration (G's)/Time (sec)	<u>5.3</u> 0.16	<u>4.1</u> 0.19	<u>7.0</u> 0.070	<u>6.2</u> 0.113	not available	<u>9.4</u> 0.25
Peak Longitudinal Acceleration (G's)/Time (sec)	<u>2.8</u> 0.08	<u>1.4</u> 0.07	<u>5.0</u> 0.080	<u>2.8</u> 0.058	<u>12.0</u> 0.13	<u>11.0</u> 0.103
Highest Average Lateral Acceleration (G's)/Time Period (sec)	<u>3.2</u> .14-.19	<u>3.6</u> .045-.095	<u>4.7</u> .17-.22	<u>4.8</u> .173-.223	not available	<u>7.2</u> 0.23-0.28
Highest Average Longitudinal Acceleration (G's)/Time Period (sec)	<u>1.0</u> .045-.095	<u>1.2</u> .045-.095	<u>2.5</u> .035-.085	<u>2.6</u> .048-.098	<u>10.0</u> 0.10-0.15	<u>10.0</u> .088-.138

* Right frame member

TABLE 3. PARAMETRIC STUDY RESULTS, MBGF

RUN NO.	IMPACT CONDITIONS		EXIT ANGLE ¹ (deg)	MAXIMUM ROLL ANGLE (deg)	MAXIMUM AVERAGE ACCELERATIONS (G's) ²		MAXIMUM SEVERITY ³ INDEX (S.I.)
	SPEED (mph)	ANGLE (deg)			G _{Long}	G _{Lat}	
1	50	5	1.9	1.8	0.56	1.92	0.39
2	50	15	5.1	5.0	2.45	4.14	0.90
3	50	25	12.2	9.6	7.80	5.50	1.57
4	70	5	1.2	1.5	0.76	2.70	0.55
5	70	15	2.9	2.3	2.87	5.51	1.15
6	70	25	7.8	10.1	12.03	8.98	2.49
7	80	5	1.0	1.6	0.88	3.15	0.64
8	80	15	2.7	3.0	3.41	6.60	1.39
9	80	25	7.0	9.7	15.30	11.53	3.17
10	60	8	2.5	1.8	1.20	3.60	0.73
11	63.4	14.7	3.6	5.0	2.59	4.80	0.98
12	57.3	25.0	9.2	8.4	9.03	6.83	1.88

¹ Angle when vehicle lost contact with barrier.

² Averaged over 50 milliseconds, at C.G. The maximum average longitudinal and lateral accelerations do not necessarily occur during the same time period.

³ As computed over 50 milliseconds.

TABLE 4. PARAMETRIC STUDY RESULTS, CMB (1)

RUN NO.	IMPACT CONDITIONS		EXIT ANGLE ¹ (deg)	MAXIMUM ROLL ANGLE (deg)	MAXIMUM AVERAGE ACCELERATIONS (G's) ²			MAXIMUM SEVERITY ³ INDEX (S.I.)
	SPEED (mph)	ANGLE (deg)			G _{Long}	G _{Lat}	G _{Vert}	
1	50.0	5.0	1.1	1.3	0.49	1.61	0.12	0.33
2	70.0	5.0	0.3	2.2	0.72	2.53	0.43	0.52
3	80.0	5.0	0.1	3.3	0.21	2.90	0.54	0.58
4	50.0	10.0	2.5	4.2	1.13	2.99	0.94	0.64
5	70.0	10.0	1.2	19.5	0.16	5.06	2.03	1.07
6	80.0	10.0	1.2	34.6	1.92	6.42	2.61	1.38
7	50.0	15.0	3.6	15.0	0.47	4.29	1.38	0.91
8	70.0	15.0	(⁴)	(⁴)	2.81	6.44	3.16	(⁴)
9	80.0	15.0	(⁴)	(⁴)	3.24	7.49	3.29	(⁴)
10	50.0	25.0	(⁵)	(⁵)	4.45	7.41	4.28	1.76
11	63.0	25.0	5.1	37.0	6.47	11.23	4.38	2.54
12	70.0	25.0	(⁵)	(⁵)	9.37	12.27	1.78	2.81

¹ Angle when vehicle lost contact with barrier.

² Averaged over 50 milliseconds, at C.G. The maximum average longitudinal and lateral accelerations do not necessarily occur during the same time period.

³ As computed over 50 milliseconds.

⁴ Vehicle rolled over upon exiting from barrier. Severity considered intolerable.

⁵ Data unavailable.

TABLE 5. ESTIMATES OF DAMAGE COSTS FOR
60 mph IMPACT (DOLLARS)

	IMPACT ANGLE					
	7 Degrees		15 Degrees		25 Degrees	
	MBGF	CMB	MBGF	CMB	MBGF	CMB
Barrier Damage	NIL	NIL	530.00 ¹	NIL	530.00 ¹	NIL
Vehicle Damage ²	490.00	615.00	1330.00	1550.00	1430.00	1500.00

¹ Taken from reference 3 with a factor of 1.2 being applied for increases in cost.

² As obtained from an auto appraiser.

TABLE 6. SEVERITY INDEX OF BARRIERS AT
60 mph IMPACT SPEED

IMPACT ANGLE (deg)	SEVERITY INDEX	
	MBGF	CMB
5	0.47	0.42
15	0.96	1.18
25	2.00	2.39

TABLE 7. SELECTION GUIDELINES

<u>MEDIAN WIDTH</u>	<u>BARRIER TYPE</u>
UP TO 18 FEET	CONCRETE
18 TO 24 FEET	CONCRETE OR DOUBLE STEEL BEAM
24 TO 30 FEET	DOUBLE STEEL BEAM